ADVANCED FUNCTIONAL MATERIALS

Supporting Information

for *Adv. Funct. Mater.*, DOI: 10.1002/adfm.202005000

Heterostructure Design in Bimetallic Phthalocyanine Boosts Oxygen Reduction Reaction Activity and Durability

Yao Ma, Jiantao Li, Xiaobin Liao, Wen Luo, Wenzhong Huang, Jiashen Meng, Qiang Chen, Shibo Xi, Ruohan Yu, Yan Zhao, Liang Zhou,* and Liqiang Mai**

Supporting Information

Heterostructure design in bimetallic phthalocyanine boosts oxygen reduction reaction activity and durability

Yao Ma, Jiantao Li, Xiaobin Liao, Wen Luo, Wenzhong Huang, Jiashen Meng, Qiang Chen, Shibo Xi, Ruohan Yu, Yan Zhao, Liang Zhou,* and Liqiang Mai**

Y. Ma, Dr. J. T. Li, X. B. Liao, Dr. W. Luo, W. Z. Huang, Dr. J. S. Meng, Q. Chen, R. H. Yu, Prof. L. Zhou, Prof. L. Q. Mai
State Key Laboratory of Advanced Technology for Materials Synthesis and Processing, Wuhan University of Technology, Wuhan 430070, P. R. China

Prof. L. Zhou, Prof. L. Q. Mai
Foshan Xianhu Laboratory of the Advanced Energy Science and Technology Guangdong Laboratory, Xianhu hydrogen Valley, Foshan 528200, China
E-mail: mlq518@whut.edu.cn (Prof. L. Q. Mai), liangzhou@whut.edu.cn (Prof. L. Zhou)

X. B. Liao, Prof. Y. Zhao
State Key Laboratory of Silicate Materials for Architectures, International School of Materials Science and Engineering, Wuhan University of Technology, Wuhan 430070, P. R. China
E-mail: yan2000@whut.edu.cn (Prof. Y. Zhao)

Dr. S. B. Xi
Institute of Chemical and Engineering Sciences, A*STAR, 1 Pesek Road, Jurong Island 627833, Singapore

Experimental Section

Material synthesis: The heterostructured Fe/Co phthalocyanine microrods were obtained by a solvothermal method. 200 mg of FePc and CoPc with different mass ratios (FePc:CoPc = 1:3, 1:1, 3:1) were dispersed into 70 mL N,N-dimethylformamide (DMF) through ultrasonication. Next, the homogeneous solution was transferred into a 100 mL teflon-lined stainless steel autoclave and heated at 180 ^{o}C for 24 h. After autoclave cooling down to room temperature, the purple precipitates were collected, washed with ethanol for 3 times, and dried. Finally, the obtained intermediate was calcined at 450 ^{o}C for 3 hours to obtain the FePc/CoPc HS.

Characterizations: To characterize the crystal properties of the samples, XRD was carried out using a Bruker D8 Discover X-ray diffractometer equipped with a Cu Kα radiation source. SEM images were detected by a JEOL-7100F scanning electron microscope. TEM images were collected by a Titan G2 60-300 with image corrector and EDX spectra were recorded using an Oxford IE250 system. XPS tests were measured on an ESCALAB 250Xi instrument. FT-IR was conducted on a Therno Nicolet Nexus instrument. ESR mesurments were collected on a JESFA200 instrument.

Electrochemical measurements: ORR performance was measured on RDE/RRDE instrument equipped with a CHI 760D electrochemical station. The results were collected in O_2 saturated 0.1 M KOH aqueous solution via three-electrode system, which was consisted of a saturated calomel electrode (SCE) as reference electrode, platinum black electrode as counter electrode, and glass carbon disk electrode of RDE (diameter = 5.0 mm) as work electrode. The ink was prepared by dispersing 5 mg of active electrocatalyst and 5 mg of VXC-72R in 800 μL of isopropyl alcohol, 150 μL of deionized water, and 50 μL of 5 wt% nafion. Then, 10 μL ink was dropped on the center of the glassy carbon dish electrode, the work electrode was obtained after the ink was dried.

All testing data were converted to reversible hydrogen electrode (RHE) via Nernst equation: $E_{RHE} = E_{SCE} + (0.24 + 0.0592\ pH)$ before analyzing.

Electron transfer number was calculated following Koutecky-Levich equation:

$$\frac{1}{j} = \frac{1}{j_L} + \frac{1}{j_K} = \frac{1}{0.62nFC_0(D_0)^{2/3}v^{-1/6}\omega^{1/2}} + \frac{1}{nFkC_0} \quad (1)$$

where j_L is diffusion-limiting current density, j_K is kinetic current density, n is electron transfer number, F is the faraday constant; C_0 is the saturated concentration of O_2 in 0.1 M KOH; D_0 is the diffusion coefficient of O_2; v is the kinetic viscosity of solution, and ω is the rotating speed of the electrode. In this part, since j_L and j_K were detected, the n could be calculated.

RRDE results could evaluate peroxide yields (HO_2^-, %) and electron transfer number (n) via the following equations:

$$n = 4\frac{I_d}{I_d + I_r / N} \quad (2)$$

$$HO_2^- = 200\frac{I_r / N}{I_d + I_r / N} \quad (3)$$

where I_r is the ring current, I_d is the disk current, and N is the collection efficiency of Pt ring electrode of RRDE (0.37).

Fabrication of primary Zn-air battery: The primary Zn-air battery was assembled with three parts. First of all, 33.66 g KOH and 2.72 g $ZnCl_2$ were dissolved in 100 mL deionized water as electrolyte. Next, a polished zinc plate (1 cm in diameter) was used as anode. Then, the air cathode was prepared by loading catalyst ink on a hydrophobic carbon cloth substrate (1 cm in diameter) with a gas diffusion layer. The catalyst ink was prepared by using the same recipe as previous ORR tests except the loading mass (1 mg cm^{-2}) on the substrate. At last, a customized electrochemical cell was adopted to assemble the mentioned parts to be a primary

Zn-air battery. All the tests were conducted in the air condition without extra oxygen pumped in. The electrochemical data were put forward without IR correction.

XAFS measurements: XANES and EXAFS experiments were conducted on the XAFCA beamline of Singapore Synchrotron Light Source. [1] The obtained EXAFS data were processed according to the procedures using ATHENA software package. [2] The k^3-weighted EXAFS was acquired through deducting the post-edge background and normalizing the related edge-jump step. After that, k^3-weighted $\chi(k)$ of Co K-edge and Fe K-edge went through Fourier transformation to the R space.

DFT caculations: The FePc, CoPc, and Fe-CoPc slabs containing 114 atoms were created to investigate the coupling effect of FePc-CoPc heterostructure. The parameters of the slabs were a=b=c= 20 Å, α=β=γ= 90. The structural relaxations were performed using the VASP (Vienna Ab-initio Simulation Package). Perdew-Burke-Ernzerhof (PBE) generalized gradient approximation (GGA) was carried out for the approximation of electronic exchange-correlation functional. The energy cutoff for the plane wave expansion method was chosen to 520 eV. Brillouin zone sampling was set to 1×1×1. Energy difference for SCF tolerance was set as 1.0×10^{-5} eV/atom for the convergence. The maximum force tolerance was set as 0.02 eV/Å for structural relaxation. The DFT-D3 method with damping was selected to acccount for the contribution of van der Waals dispersion energies.

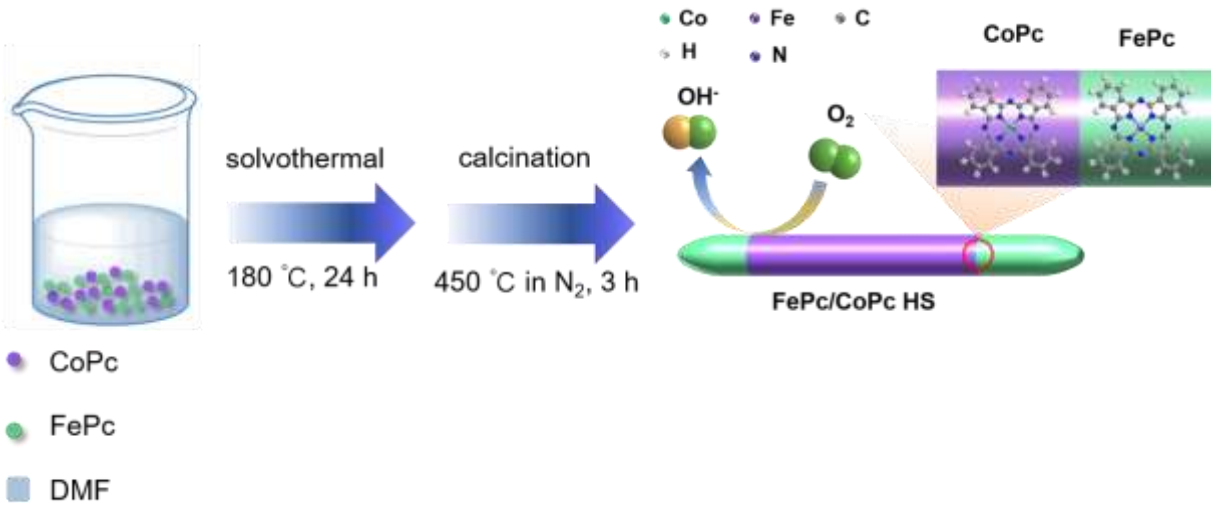

Figure S1. Synthetic schematic of FePc/CoPc HS.

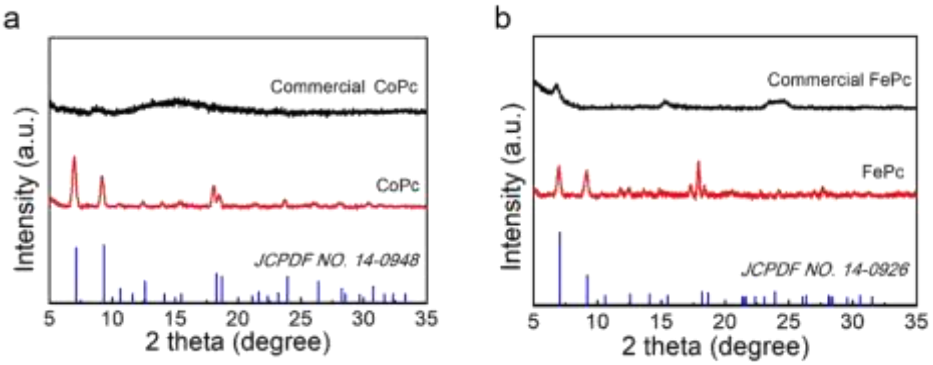

Figure S2. XRD patterns of a) CoPc and b) FePc.

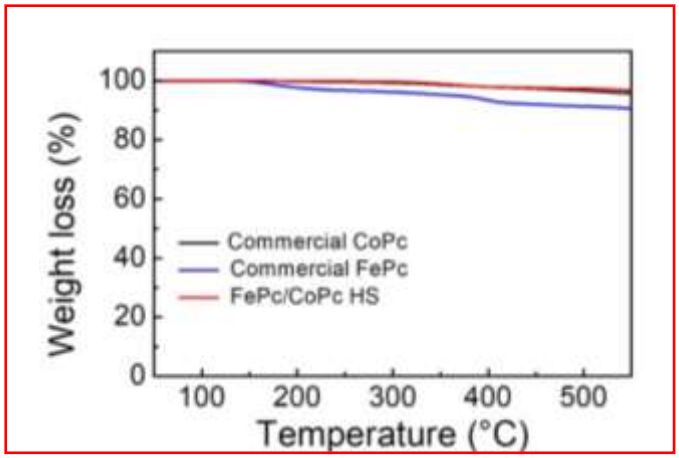

Figure S3. TG curves of commercial CoPc, commercial FePc and FePc/CoPc HS.

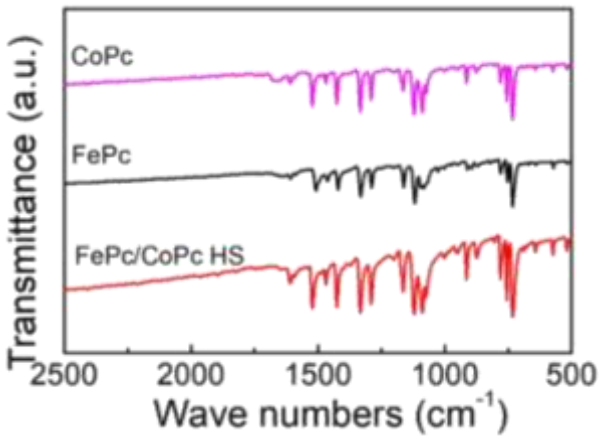

Figure S4. FT-IR spectra of CoPc, FePc, and FePc/CoPc HS.

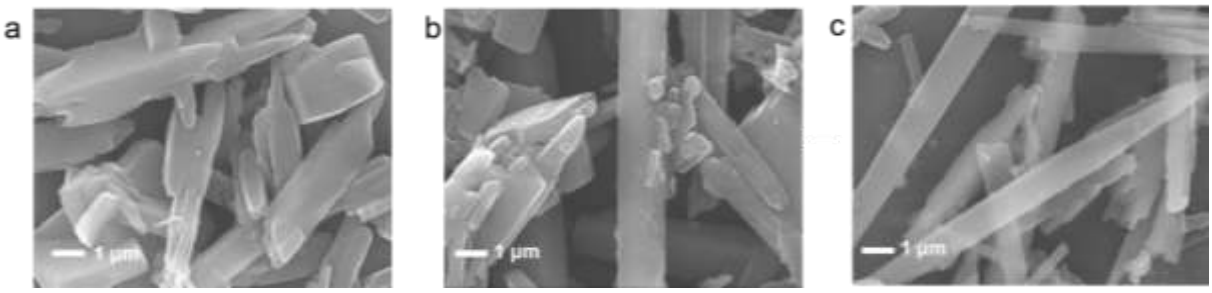

Figure S5. SEM images of a) CoPc, b) FePc, and c) FePc/CoPc HS.

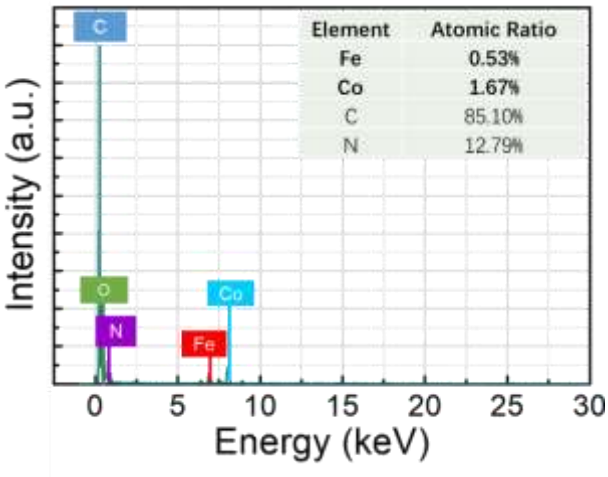

Figure S6. EDS spectrum of FePc/CoPc HS showing the elemental composition.

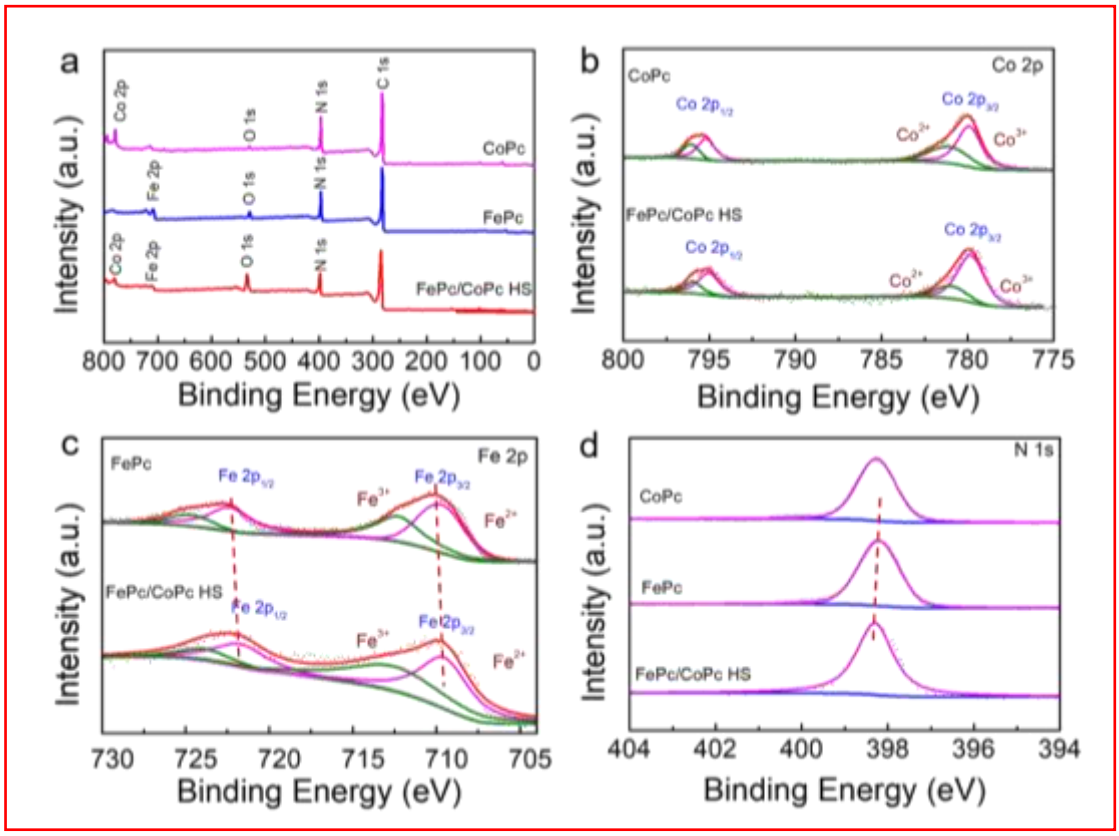

Figure S7. XPS spectra of CoPc, FePc, and FePc/CoPc HS. a) Full survey, b) Co 2p, c) Fe 2p, d) N 1s spectra.

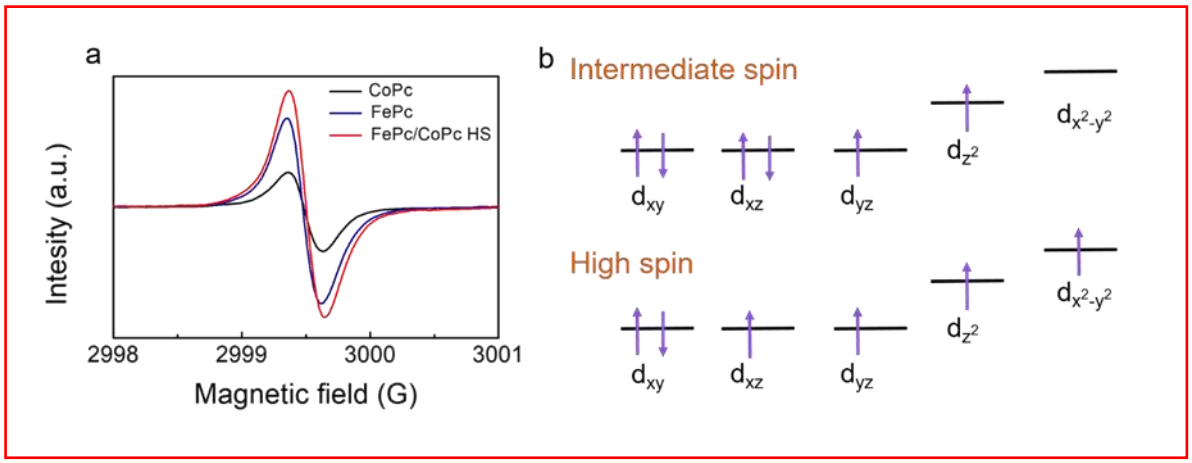

Figure S8. a) ESR spectra of CoPc, FePc and FePc/CoPc HS. b) Schematic of the spin transition of Fe(II) in FePc/CoPc HS.

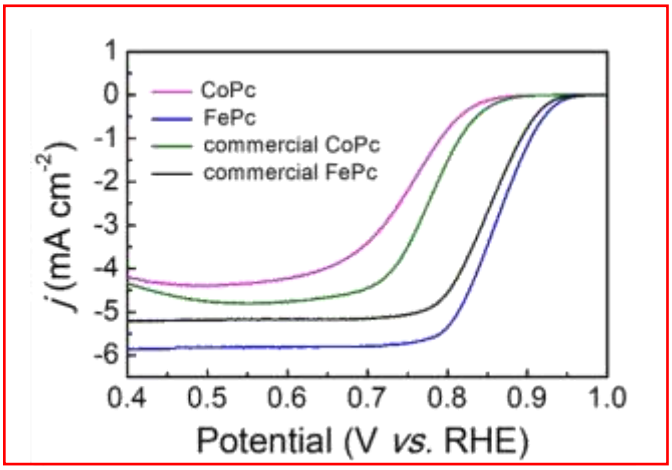

Figure S9. LSV curves of as-prepared CoPc, FePc, and commercial CoPc, FePc.

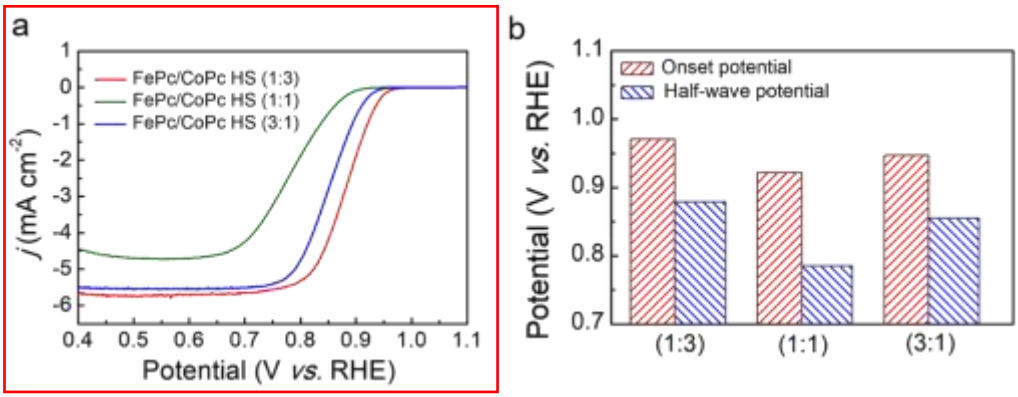

Figure S10. a) LSV curves and b) comparison diagrams of onset potential and half-wave potential of FePc/CoPc HS with different mass ratios.

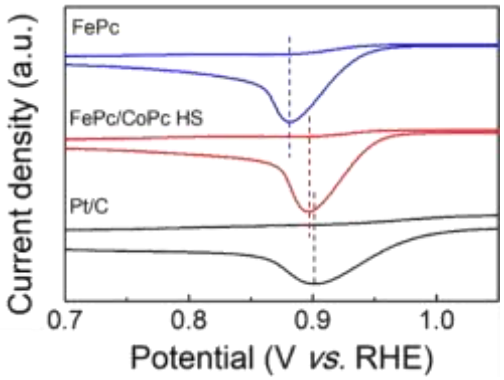

Figure S11. Cyclic voltammograms of FePc/CoPc HS, FePc, and Pt/C at a scan rate of 5 mV s^{-1}.

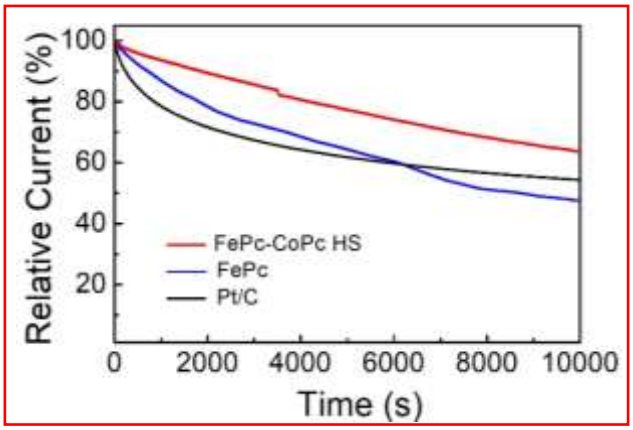

Figure S12. Chronoamperometric responses of FePc/CoPc HS, FePc, and Pt/C at 1000 rpm at half-wave potential.

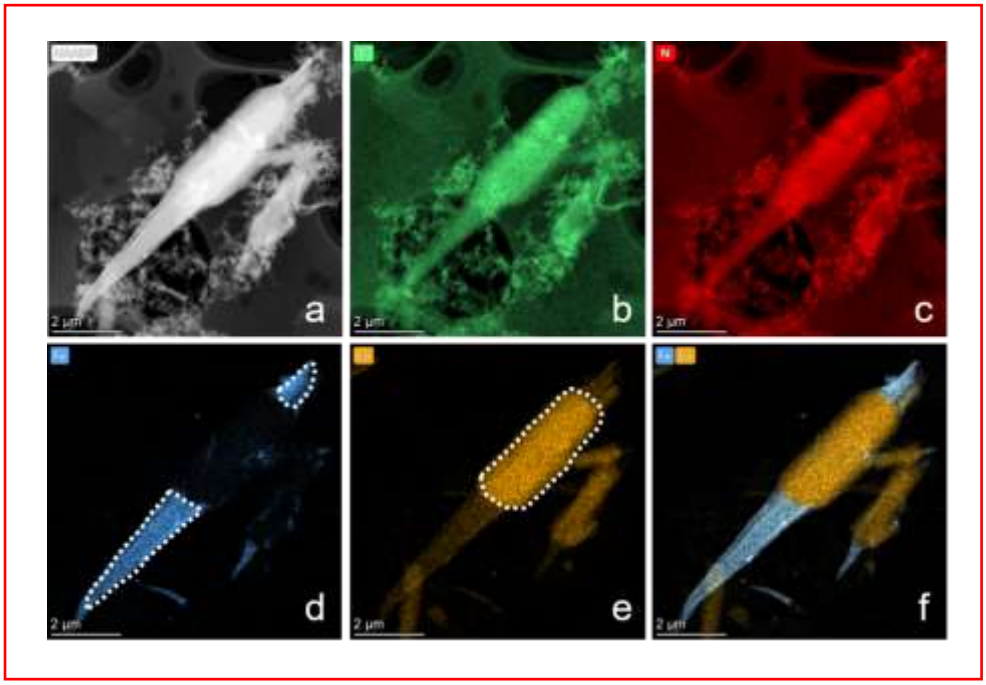

Figure S13. The HAADF-STEM image and the corresponding EDS mappings of FePc/CoPc HS after 5000 s stability test.

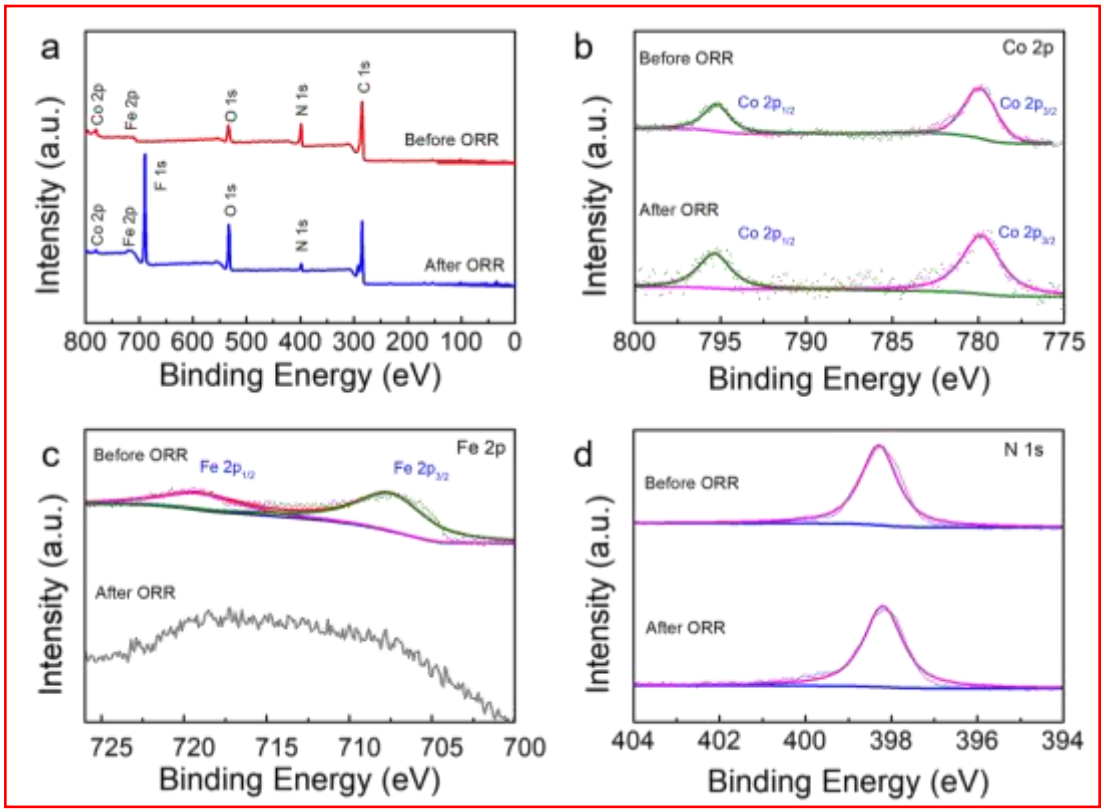

Figure S14. XPS spectra of FePc/CoPc HS and corresponding catalysts after 5000 s stability test. a) Full survey, b) Co 2p, c) Fe 2p, d) N 1s.

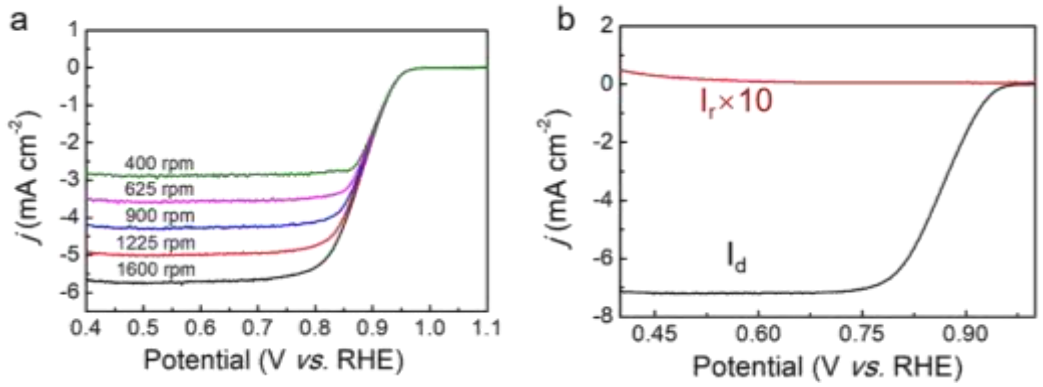

Figure S15. a) LSV curves of FePc/CoPc HS at different rotating speeds from RDE. b) LSV curves of FePc/CoPc HS from RRDE.

Table S1. Electrochemical performance comparison of phthalocyanine-based catalysts.

Materials	Onset Potential (V)	Half-wave Potential (V)	Limiting Diffusion Current Density (mA cm^{-2})	References
FePc/CoPc HS	[a]0.971	[a]0.879	5.71	This work
FePc-G	[a]0.960	[a]0.838	/	[3]
FePc-CNTs	[a]0.864	[a]0.77	5.33	[4]
$Fe_{0.5}Co_{0.5}$Pc-CP	[a]0.937	[a]0.848	5.98	[5]
PcCu-O_8-Co	/	[a]0.83	5.3	[6]
NP-Fe-HPC (FePc-based)	/	[a]0.82	5.2	[7]
NDC-900_Fe (FePc-based)	[b]0.83	[b]0.76	/	[8]
FePc-PcFe	[c]0.8	[c]0.59	/	[9]
CoPc-SO_3H/CNT	[a]0.88	[a]0.78	4.60	[10]
MWNT/FePc-SH	[a]0.971	[a]0.856	/	[11]

a: the electrolyte are 0.1 M KOH; b: the electrolyte are 0.05 M H_2SO_4; c: b: the electrolyte are 0.1 M $HClO_4$

Reference in Supporting Information

[1] Y. Du, Y. Zhu, S. Xi, P. Yang, H. O. Moser, M. B. H. Breese, A. Borgna, *J. Synchrotron Radiat* **2015**, *22*, 839.

[2] B. Ravel, M. Newville, *J. Synchrotron Radiat* **2005**, *12*, 537.

[3] Y. Cheng, X. Wu, J.-P. Veder, L. Thomsen, S. P. Jiang, S. Wang, *Energy Environ. Mater.* **2019**, *2*, 5.

[4] X. Yan, X. Xu, Z. Zhong, J. Liu, X. Tian, L. Kang, J. Yao, *Electrochim. Acta* **2018**, *281*, 562.

[5] W. Liu, Y. Hou, H. Pan, W. Liu, D. Qi, K. Wang, J. Jiang, X. Yao, *J. Mater. Chem. A* **2018**, *6*, 8349.

[6] H. Zhong, K. H. Ly, M. Wang, Y. Krupskaya, X. Han, J. Zhang, J. Zhang, V. Kataev, B. Buchner, I. M. Weidinger, S. Kaskel, P. Liu, M. Chen, R. Dong, X. Feng, *Angew. Chem. Int. Ed.* **2019**, *58*, 10677.

[7] Z. Zhang, J. Sun, F. Wang, L. Dai, *Angew. Chem. Int. Ed.* **2018**, *57*, 9038.

[8] A. Mehmood, J. Pampel, G. Ali, H. Y. Ha, F. Ruiz-Zepeda, T.-P. Fellinger, *Adv. Energy Mater.* **2018**, *8*, 1701771.

[9] X. Wang, Y. Liu, Y. Wang, R. Ren, H. Chen, Z. Jiang, Q. He, *ChemElectroChem* **2018**, *5*, 3478.

[10] C. Li, T. Huang, Z. Huang, J. Sun, C. Zong, J. Yang, W. Deng, F. Dai, *Dalton Trans.* **2019**, *48*, 17258.

[11] J. Yang, F. Toshimitsu, Z. Yang, T. Fujigaya, N. Nakashima, *J. Mater. Chem. A* **2017**, *5*, 1184.